VEGF receptor signaling links inflammation and tumorigenesis in colitis-associated cancer

Maximilian J. Waldner,[1,2] Stefan Wirtz,[1,2] André Jefremow,[2] Moritz Warntjen,[2] Clemens Neufert,[1] Raja Atreya,[1] Christoph Becker,[1,2] Benno Weigmann,[1,2] Michael Vieth,[3] Stefan Rose-John,[4] and Markus F. Neurath[1,2]

[1]Department of Medicine I, University of Erlangen-Nuremberg, D-91054 Erlangen, Germany
[2]Institute of Molecular Medicine, University of Mainz, D-55131 Mainz, Germany
[3]Institute of Pathology, Klinikum Bayreuth, D-95445 Bayreuth, Germany
[4]Department of Biochemistry, Christian-Albrechts-Universität zu Kiel, Medical Faculty, D-23098 Kiel, Germany

The Journal of Experimental Medicine

Whereas the inhibition of vascular endothelial growth factor (VEGF) has shown promising results in sporadic colon cancer, the role of VEGF signaling in colitis-associated cancer (CAC) has not been addressed. We found that, unlike sporadic colorectal cancer and control patients, patients with CAC show activated VEGFR2 on intestinal epithelial cells (IECs). We then explored the function of VEGFR2 in a murine model of colitis-associated colon cancer characterized by increased VEGFR2 expression. Epithelial cells in tumor tissue expressed VEGFR2 and responded to VEGF stimulation with augmented VEGFR2-mediated proliferation. Blockade of VEGF function via soluble decoy receptors suppressed tumor development, inhibited tumor angiogenesis, and blocked tumor cell proliferation. Functional studies revealed that chronic inflammation leads to an up-regulation of VEGFR2 on IECs. Studies in conditional STAT3 mutant mice showed that VEGFR signaling requires STAT3 to promote epithelial cell proliferation and tumor growth in vivo. Thus, VEGFR-signaling acts as a direct growth factor for tumor cells in CAC, providing a molecular link between inflammation and the development of colon cancer.

CORRESPONDENCE
M.F. Neurath:
markus.neurath@uk-erlangen.de

Abbreviations used: AOM, azoxymethane; CAC, colitis-associated cancer; CRC, colorectal cancer; DSS, dextran sodium sulfate; IBD, inflammatory bowel disease; IEC, intestinal epithelial cell; STAT3, signal transducer and activator of transcription 3; VEGF, vascular endothelial growth factor; VEGFR, VEGF receptor.

Tumor development has been regarded as a multistep process that involves tumor initiation, promotion, and progression. Whereas tumor initiation is considered to be dependent on genetic alterations that increase survival and proliferation of single cells, various paracrine and autocrine mechanisms stimulate the growth of these initiated tumor cells during tumor promotion, and the growing cluster of tumor cells finally develops malignant characteristics, including invasion and metastatic growth in the course of progression (Pitot, 1993; Balkwill et al., 2005).

As the distance of individual cells to blood vessels increases during tumor growth, these cells are depleted of oxygen and nutrients and therefore depend on the recruitment of new vessels to the tumor site through angiogenesis (Ferrara, 2009). After the proposition of vascularization as an essential component of tumor growth and the inhibition of angiogenesis as a promising strategy for the treatment of cancer by Folkman (1971), subsequent research on various pro- and antiangiogenic molecules finally led to the approval of the first antiangiogenic substance, bevacizumab, for first-line treatment of metastatic colorectal cancer (CRC; Kerbel, 2008).

Bevacizumab is a humanized monoclonal antibody directed against vascular endothelial growth factor (VEGF), a molecule that has been regarded as the major mediator of tumor angiogenesis. VEGF is expressed by most types of cancer after the activation of hypoxia-inducible transcription factors 1α and 2α in response to hypoxia and metabolic stress (Semenza, 2003). Although VEGF is a ligand for VEGF receptor 2 (VEGFR2) and VEGFR1, VEGF signaling in angiogenesis is mainly mediated through VEGFR2, a receptor tyrosine kinase that is expressed at elevated levels by endothelial cells

The Rockefeller University Press $30.00
J. Exp. Med. Vol. 207 No. 13 2855-2868
www.jem.org/cgi/doi/10.1084/jem.20100438

(Shibuya and Claesson-Welsh, 2006). The activation of VEGFR2 on endothelial cells results in their proliferation, migration, and increased survival and promotes vascular permeability. Although VEGF has a 10 times higher affinity for VEGFR1 in comparison to VEGFR2, the role of VEGFR1 in angiogenesis remains to be defined (Cao, 2009).

In addition to tumor development, growing evidence supports a role for angiogenesis and VEGF in the pathogenesis of chronic inflammatory disorders such as rheumatoid arthritis, psoriasis, and inflammatory bowel disease (IBD; Costa et al., 2007). VEGF is not only released by various cells of the immune system at the site of inflammation to induce angiogenesis but also directly activates immune cells as part of a positive feedback loop (Yoo et al., 2008; Scaldaferri et al., 2009).

Interestingly, chronic inflammation markedly increases the risk for the development of cancer, as seen in patients with IBD (Clevers, 2004; Zisman and Rubin, 2008), and therefore angiogenesis and VEGF signaling might pose an important link between inflammation and tumor development. However, the molecular mechanisms that lead to cancer in chronic inflammation and the role of angiogenesis in inflammation-associated cancer remain poorly understood.

In the present study, we analyzed the role of angiogenesis and VEGF signaling in a mouse model of colitis-associated cancer (CAC) using azoxymethane (AOM) and dextran sodium sulfate (DSS) to study the interplay between inflammation, angiogenesis, and VEGF signaling during tumor development. In these studies, tumor growth was paralleled by alterations of the microvascular architecture and increased expression of VEGF and VEGFR2. Furthermore, inhibition of VEGF signaling through administration of VEGF-Trap, a soluble decoy receptor made from extracellular domains of VEGFR1 and VEGFR2, or an adenoviral vector expressing sVEGFR1, reduced tumor growth. Tumor cells highly expressed VEGFR2, and activation of this receptor resulted in increased tumor proliferation in a STAT3-dependent manner. The up-regulation of VEGFR2 could not only be observed on tumor cells but also on intestinal epithelial cells (IECs) during colitis and was mediated by the proinflammatory cytokine IL-6, which has been shown to be a strong promoter of tumor growth in experimental CAC (Becker et al., 2004).

These data suggest that VEGF acts as a direct link between inflammation and cancer development, and provide a rationale for the use of anti-VEGF therapeutics in chronic IBDs with an increased risk of tumor development. Additionally, cancer response rates to anti-VEGF therapeutics might be influenced by VEGFR2 expression on the tumor cells themselves.

RESULTS

VEGFR2 is up-regulated on vascular endothelial cells and epithelial cells in mouse and human CAC

Although VEGF signaling has been identified as key factor in the pathogenesis of sporadic colorectal tumors in mice and humans (Jain et al., 2006; Boquoi et al., 2009; Grothey and Galanis, 2009), little is known about the function of VEGF in colitis-associated tumors. To analyze the role of VEGF signaling in colitis-associated neoplasias, we exposed wild-type mice to a mouse model of CAC using AOM+DSS (Fig. 1 A). In these experiments, significantly elevated levels of VEGF were detected in the plasma and tumor tissue of tumor-bearing mice as compared with control mice (Fig. 1 B). Furthermore, VEGFR2 mRNA expression was increased in tumor cells (Fig. 1 C) and VEGFR2 protein levels were elevated in the inflamed colon and tumors of AOM+DSS-treated animals as compared with control animals (Fig. 1 D). Subsequent studies aiming at the identification of cells expressing VEGFR2 revealed marked VEGFR2 expression on IECs from tumor tissue, whereas little or no VEGFR2 expression was seen on control IECs (Fig. 1, D and E). Consistently, IECs isolated from tumors expressed significantly higher amounts of VEGFR2 mRNA as compared with control IECs (Fig. S1 A). Collectively, these findings indicated the expression of VEGFR2 on IECs from tumor tissue in AOM+DSS colitis.

To further analyze the expression of VEGF and VEGFR2 during the course of AOM+DSS colitis, we exposed transgenic mice with a luciferase reporter driven by the promoter for VEGF or VEGFR2 to the AOM+DSS protocol. In these mice, VEGF and VEGFR2 promoter activity was paralleled by intestinal inflammation with strong luminescence signals in the whole abdominal region, suggesting a role for VEGF and VEGFR2 signaling before tumor development (Fig. 1 F). Quantification of luminescence revealed a significant induction of both VEGF and VEGFR2 promoter activity in AOM+DSS-treated mice during the course of the disease (Fig. 1 F).

To identify the cellular source of VEGFR2 expression, we performed immunohistochemical double staining for VEGFR2 with markers of IECs (E-Cadherin), vascular endothelial cells (CD31), granulocytes (MPO), macrophages (F4/80), and $CD4^+$ T cells. In these studies, expression of VEGFR2 in colitis-associated neoplasias was seen on CD31-expressing cells. In contrast, F4/80 and CD4-expressing cells showed little or no staining for VEGFR2. Furthermore, we noted marked expression of VEGFR2 on IECs in tumor tissue, whereas IECs in control mucosa showed no staining (Fig. 2; Fig. S1 B for controls). VEGFR2 expression was mainly localized at the basolateral membrane of tumor IECs. In contrast to VEGFR2, no staining of IECs was noted with an anti-VEGFR1 antibody, although some stroma cells showed staining for VEGFR1 (Fig. S1 C).

To further evaluate a functional role for VEGFR2 on IECs, we performed immunohistochemistry for phospho-VEGFR2 (pVEGFR2) and E-Cadherin. It was found that pVEGFR2 is expressed on tumor epithelial cells in AOM+DSS-treated mice (Fig. 2), consistent with the idea that functionally active VEGFR2 is expressed by IEC in colonic tumors. In addition to VEGFR2, we analyzed the expression of VEGF in various cell subsets using immunohistochemical double staining. VEGF was expressed in IECs and stroma cells, suggesting an activation of the VEGF–VEGFR2 pathway in AOM+DSS-treated animals (Fig. S2 A).

Because a role for VEGFR2 on IEC has not been described so far in human intestinal inflammation and tumor development, we additionally conducted immunohistochemistry

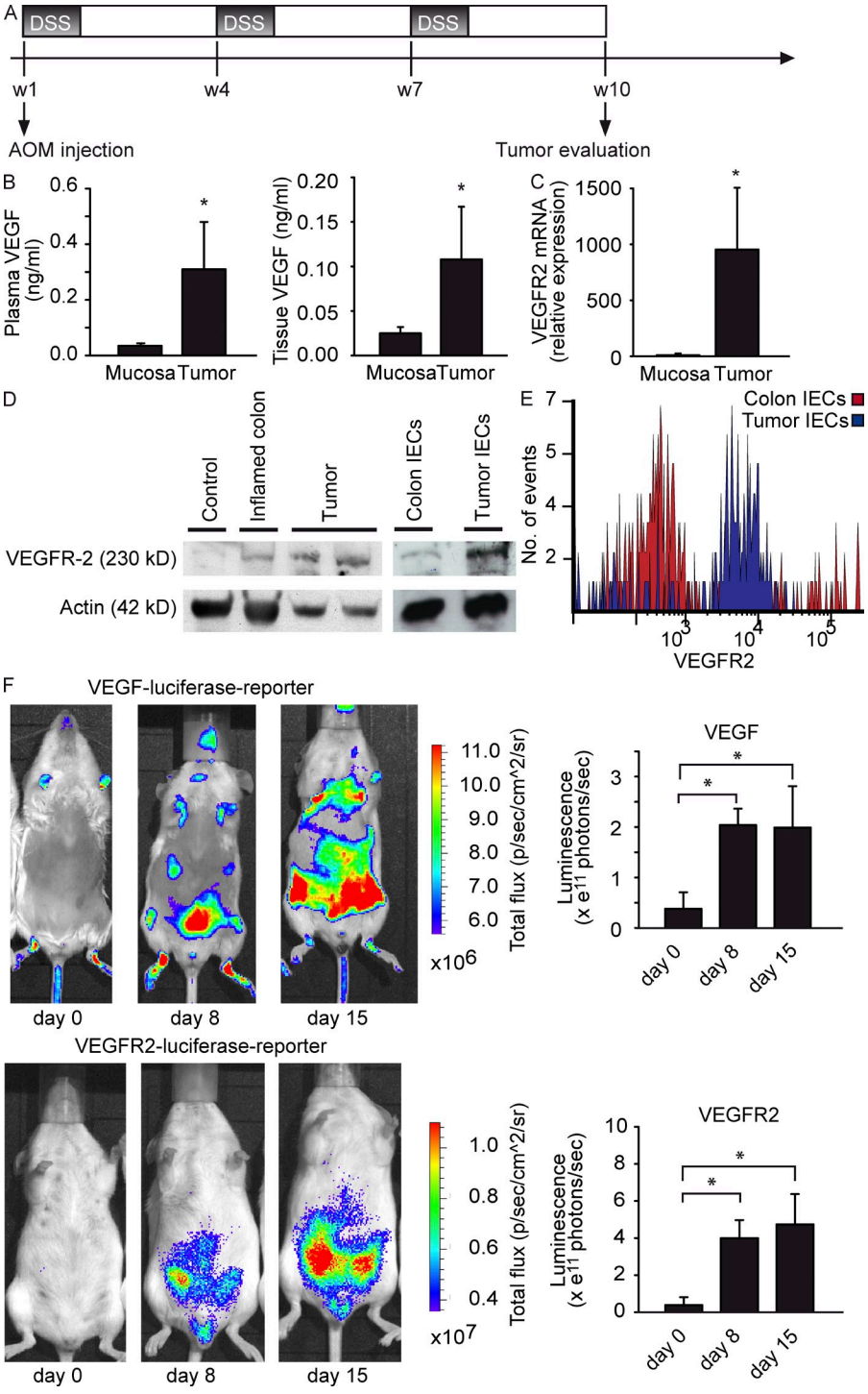

Figure 1. Up-regulation of VEGF and VEGFR2 expression through intestinal inflammation in the AOM+DSS-induced mouse model of CAC. (A) Mouse CAC is induced through the injection of AOM at day one, followed by three cycles of DSS in the drinking water and two weeks with normal drinking water. (B) Plasma and tissue levels of VEGF were analyzed from AOM+DSS-treated animals at indicated time points. Data show mean values ± SD (n = 5 per group) and are representative of two different experiments. Furthermore, tissue VEGF is increased in tumors in comparison to healthy mucosa. Data represent mean values ± SD (n = 7 per group). *, $P < 0.05$. (C) Quantitative PCR of VEGFR2 mRNA in tumor cells and normal epithelial cells of untreated animals. Data represent mean values ± SD (n = 4 per group) and are relative to Hprt1 mRNA. The experiment was performed twice with similar results. *, $P < 0.05$. (D) Protein lysates from control colon, inflamed colon, and tumor tissue of AOM+DSS-treated mice were analyzed by immunoblot. Actin served as loading control. Data are representative of three independent experiments. (E) FACS analysis of isolated IECs from tumor and control tissue. IECs were isolated as specified in Material and methods and stained for E-Cadherin and VEGFR2. Histograms are gated on E-Cadherin$^+$ cells. One representative experiment out of three is shown. (F) Transgenic mice with a luciferase reporter driven by the promoter for VEGF (top) or VEGFR2 (bottom) were treated with AOM+DSS. Top images show one representative mouse out of nine independent experiments at several time points. Luminescence is illustrated with photons/sec/cm^2/sr as indicated by the false-color chart. (bottom) Quantification of data was performed by analyzing the total flux of photons/second in the abdominal regions of experimental animals at indicated time points. Data represent mean values ± SD (n = 8 per group). *, $P < 0.05$.

for VEGFR2 and pVEGFR2 on human tissue samples obtained from patients with IBD (Crohn's disease and ulcerative colitis), CAC, and sporadic CRC in comparison to control samples. Whereas VEGFR2 expression was restricted to endothelial cells in control tissue, we found an increased expression of VEGFR2 in IBD and CAC, and this increase was more pronounced as compared with CRC (Fig. 3 A). Again, VEGFR2 expression in IBD patients could be observed on IECs, whereas VEGFR2 was mainly restricted to endothelial cells in healthy mucosa and CRC. In contrast to VEGFR2, no staining for VEGFR1 on human IECs in IBD and CAC was noted (Fig. S1 D).

In addition, marked expression of pVEGFR2 on IECs was observed in IBD and CAC (Fig. 3 B), whereas increased expression of VEGF was noted in stroma cells and IECs in IBD and CAC patients (Fig. S2 B). The expression of VEGFR2 on epithelial cells might be a consequence of chronic inflammation as observed in IBD and CAC patients consistent with the hypothesis that activation of this receptor on epithelial cells might have a previously unrecognized function.

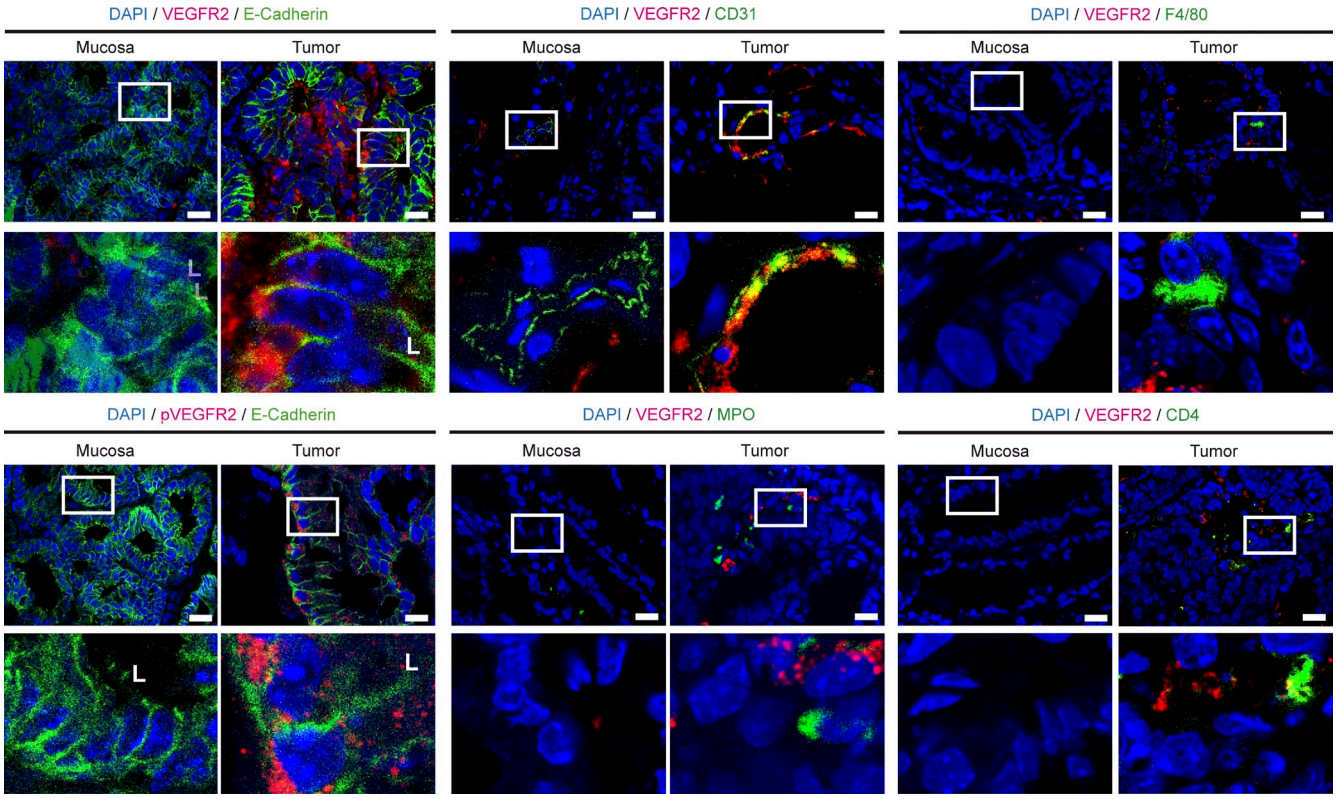

Figure 2. VEGFR2 is up-regulated and activated in tumor cells in a mouse model of CAC. Tumors and normal mucosa of AOM+DSS-treated animals were analyzed by confocal microscopy with antibodies specific for the indicated proteins. L, luminal side of intestinal crypt. Images show representative images out of five experiments. Bars, 25 µm.

The inhibition of VEGF-signaling reduces tumor growth in experimental CAC

In subsequent experiments, we aimed at the functional characterization of VEGF by blocking VEGF activity in vivo. In these studies, we used optical contrast endoscopy, a technique that is increasingly being used in the clinics for the diagnosis of intestinal tumors upon endoscopy (Emura et al., 2008). Optical contrast endoscopy enabled us to detect alterations of the vessel architecture at an early stage, small neoplastic lesions, and thereby facilitated identification and quantification of tumors (Fig. S3 A). Tumors in AOM+DSS-treated mice showed enhanced expression of integrin $\alpha_v\beta_3$ (Fig. S3 B), a receptor that is involved in the regulation of angiogenesis (Avraamides et al., 2008), as demonstrated by in vivo multispectral fluorescence imaging.

To further examine the functional role of VEGF in vivo, animals were evaluated at week 4 of the AOM+DSS protocol for tumor growth using optical contrast endoscopy and allocated to groups with balanced tumor scores (Fig. 4 A). Individual groups were then treated with VEGF-Trap or soluble VEGFR1 (sVEGFR1) and their respective controls (hFc vs. VEGF-Trap/sVEGFR1 vs. LacZ expressing vector) to assess the effects of VEGF blockade on tumor growth. During the whole experimental protocol, tumor development and growth were evaluated repeatedly using high-resolution endoscopy in living mice (Becker et al., 2004). Treatment of mice with both VEGF-Trap and sVEGFR1 resulted in decreased tumor scores, mainly because of reduced tumor numbers, whereas there was no difference concerning colonic inflammation upon endoscopy between treated groups and control groups (Fig. 4 B). In addition, optical contrast endoscopy was used to detect alterations of the vessel architecture upon VEGF blockade. "Abnormal" patterns of tumor vessels are regarded as a sign of tumor angiogenesis, and antiangiogenic therapy has been shown to normalize alterations of the tumor vasculature (Jain, 2005). Optical contrast endoscopy revealed a reduced density of superficial vessels on tumors of VEGF-Trap–treated animals (Fig. 4 C).

To analyze the functional architecture of microvessels of the intestinal mucosa in more detail, we further applied confocal in vivo endoscopy of the colon after i.v. injection of the plasma marker FITC-dextran to optical contrast endoscopy (Fig. 4 C and Fig. S3 C). We used a confocal laser probe that could be fed through the working sheet of our endoscope and enabled us to directly position the probe on an area of interest and obtain microscopic pictures of the vasculature. This so-called endomicroscopy revealed a more organized architecture of the mucosal vasculature upon VEGF blockade in comparison to the more "chaotic" vessel architecture in the control group. To quantify these alterations, we used the assessment of the fractal dimension for the description of the pathological

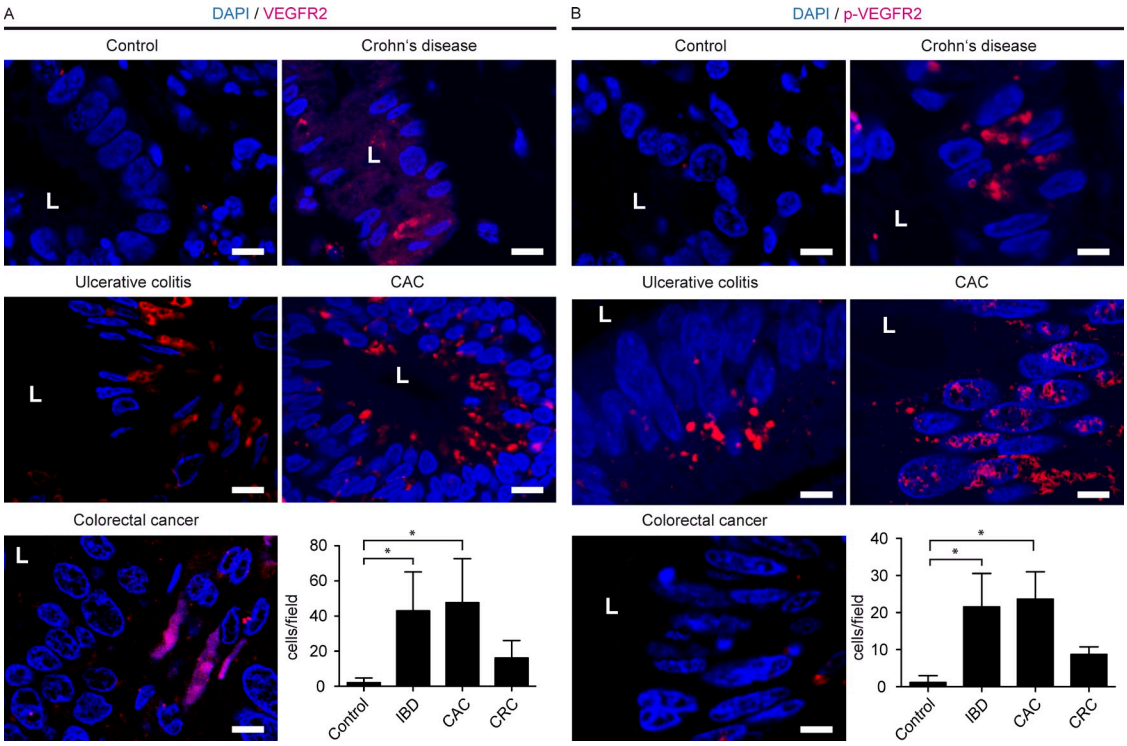

Figure 3. Colonic epithelial cells express VEFGR-2 in human IBD and CAC. Tissue sections from control patients or patients with Crohn's disease, ulcerative colitis, sporadic CRC, or CAC were analyzed by confocal microscopy with the indicated antibodies. L, luminal side of intestinal crypt. The experiments were performed twice with similar results. Bar graphs show data generated by counting VEGFR2 and pVEGFR2-positive epithelial cells. Data represent mean values ± SD (n = 4–8 per group). *, $P < 0.01$ (A); *, $P < 0.005$ (B). CRC, sporadic CRC; IBD, IBD including ulcerative colitis and Crohn's disease. Bars, 10 µm.

architecture of tumor vessels (Baish and Jain, 2000; Fig. S3 D). The fractal dimension of the normal mucosal capillary network had a mean value of 1.93 ± 0.05, which is characteristic for capillaries. In contrast, the fractal dimension of the tumor microvasculature had a mean value of 1.73 ± 0.07, which reflects the decreased order of the vessel architecture. Upon VEGF-Trap treatment, a significant reduction of the fractal dimension was found as compared with the control group, suggesting a "normalization" of the microvascular vessel architecture after functional VEGF blockade in vivo (Fig. 4 C).

Furthermore, VEGF-Trap–treated mice had a reduced integrin $\alpha_v\beta_3$ expression in the distal colon and tumors showed a significant decrease in intratumoral vessel density upon immunohistochemistry for CD31 (Figs. 4, D and E). Whereas these alterations of vessel morphology could be attributed to an antiangiogenic effect of VEGF inhibition, the reduced tumor scores could also have been a consequence of a direct effect of VEGF signaling on VEGFR2-expressing tumor cells.

VEGF induces tumor cell proliferation via activation of VEGFR2 on IECs

To further characterize effects of VEGF blockade on tumor tissue, we performed immunohistochemical double staining. Infiltrating MPO^+ granulocytes could only rarely be observed in VEGF-Trap and control groups (unpublished data). However, there was a comparable infiltration of tumors with $F4/80^+$ cells and $CD4^+$ T cells in both groups (Fig. 5 A). Furthermore, no difference in cleaved caspase-3 staining in stroma cells was noted between the groups, suggesting that VEGF-Trap does not directly control apoptosis of these cells. In contrast, a marked reduction in the number of proliferating epithelial cells was noted upon VEGF-Trap treatment, as shown by E-Cadherin/Ki67 double staining (Fig. 5 A). Quantification of $Ki67^+$ cells revealed that tumors of control animals had statistically significant higher numbers of proliferating epithelial cells in comparison to VEGF-Trap–treated animals (Fig. 5 B). As these results were consistent with the idea that VEGF directly controls proliferation of IECs in tumor tissue via VEGFR2, we incubated tumor tissues of wild-type mice exposed to the AOM+DSS protocol to VEGF (250 ng/ml) in a tissue culture. In comparison to culture medium alone, VEGF treatment increased the number of proliferating epithelial cells in tumor culture as revealed by E-Cadherin/Ki67 staining (Fig. 5 C).

To analyze the role of VEGF on epithelial cells in vivo, we injected VEGF (100 ng) or PBS three times per week into tumors of wild-type mice exposed to the AOM+DSS protocol. Similar to the aforementioned tissue culture experiments, the administration of VEGF in vivo resulted in increased tumor

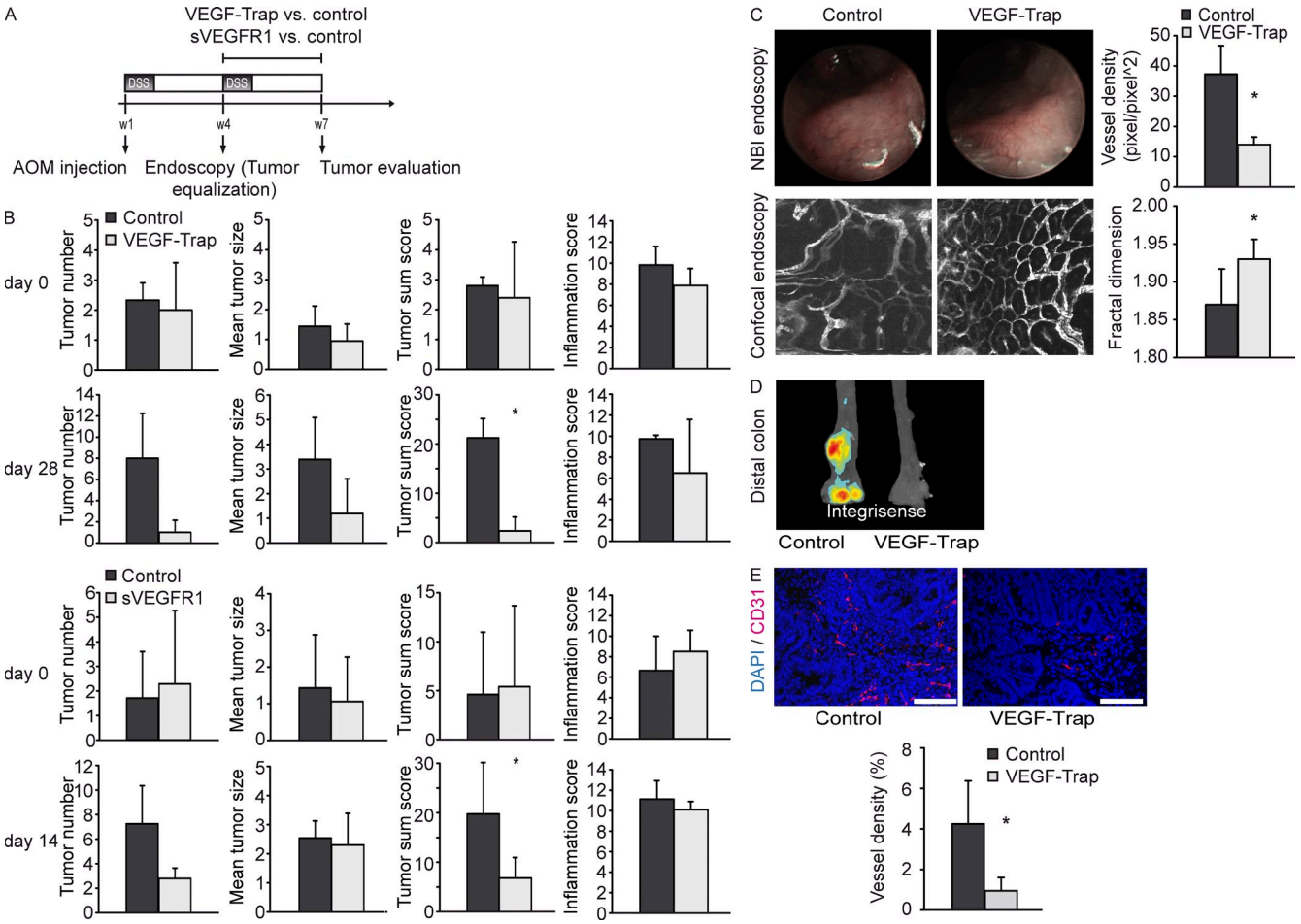

Figure 4. Anti-VEGF treatment reduces tumor growth in CAC. (A) After initial endoscopy for the detection of already established tumors after 4 wk of the AOM+DSS protocol, mice were treated with VEGF-Trap versus control (3 times per week) or a vector expressing sVEGFR1 versus control (injected once at week 5). (B) Tumor number, tumor size, and tumor inflammation were measured at the indicated time points after start of each treatment. Data represent mean values ± SD (n = 10 per group). The experiment was performed twice with similar results. (C) Mice treated or not treated with VEGF-Trap were analyzed by optical contrast endoscopy and confocal endoscopy. Fractal dimension and vessel density were measured. Representative images of five experiments are shown. Data represent mean values ± SD (n = 5 per group). *, P < 0.05. NBI, narrow band imaging. (D) Multispectral fluorescence imaging for integrin $\alpha_v\beta_3$ expression was performed in untreated and VEGF-Trap–treated animals. Representative images of five experiments are shown. (E) The intratumoral vessel density was measured in VEGF-Trap–treated and untreated animals. Representative images of five experiments are shown. Data represent mean values ± SD (n = 5 per group). *, P < 0.05. Bars, 100 µm.

growth (Fig. 6 A) and proliferation of tumor cells, as shown by Ki67 staining (Fig. 6 B). Thus, we assumed that VEGF has a direct effect on tumor proliferation, which is independent of angiogenesis.

To further evaluate whether VEGF receptor 2 is responsible for the effect of VEGF on epithelial cell proliferation, we administered VEGF to an organ culture of both murine and human inflamed colonic tissue. Administration of VEGF led to significantly increased proliferation of epithelial cells in AOM+DSS colitis and IBD patients and this increase could be suppressed through the administration of anti-VEGFR2 antibodies (Fig. 6, C and D). These data further support a direct proliferative effect of VEGF on IECs through the activation of VEGFR2. As Ki67 staining showed an increased proliferation of IECs in IBD patients (Fig. S4, A and B), our findings were consistent with the idea that VEGF signal transduction plays a role at early stages of tumor development in chronic intestinal inflammation by controlling proliferation of IECs.

VEGFR2 activation on IEC leads to STAT3 phosphorylation: STAT3 is essential for VEGF-mediated tumor growth in vivo

Recent studies have described the activation of STAT3 as a critical step during the development of cancer and CAC in particular. Concerning CAC, it has been shown that STAT3 activation can be mediated via IL-6 (Bollrath et al., 2009; Grivennikov et al., 2009). Interestingly, VEGFR2 activation has also been shown to lead to STAT3 phosphorylation on endothelial cells (Chen et al., 2008). Therefore, we examined STAT3 phosphorylation in tumors of VEGF-Trap–treated animals and controls by immunohistochemistry (Fig. 7 A). In fact,

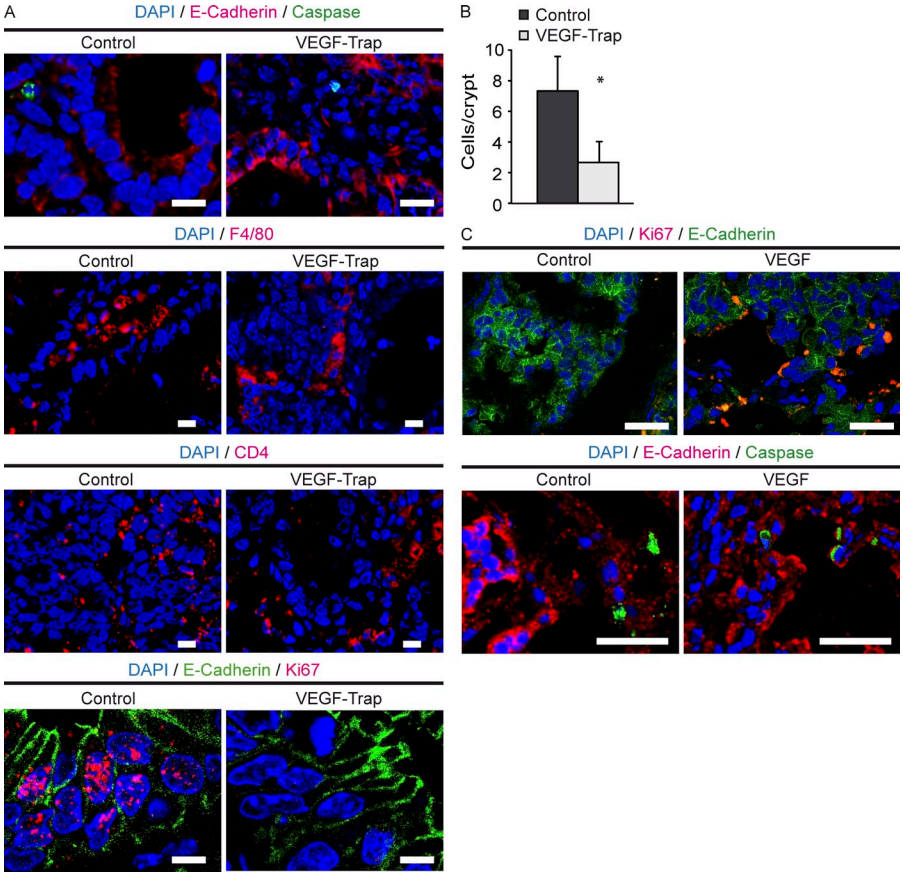

Figure 5. VEGF directly promotes the proliferation of tumor cells. (A) Colons of VEGF-Trap and control treated animals were analyzed by immunohistochemistry with antibodies specific for the indicated markers. The experiment was performed twice with similar results. (B) The number of E-Cadherin$^+$/Ki67$^+$ double-positive cells was quantified in VEGF-Trap and control groups. Data are presented as mean values of positive cells ± SD (n = 5 per group). *, $P < 0.01$. The experiment was repeated twice with similar results. (C) VEGF (250 ng/ml) was added to tissue cultures of AOM+DSS-induced tumors, and proliferation and apoptosis of tumor cells was measured after staining with the indicated antibodies. Representative images from three independent experiments are shown. Bars: (A) 10 µm; (C) 25 µm.

VEGF-Trap treatment resulted in reduced numbers of pSTAT3$^+$ cells in colonic tumors. Next, we analyzed STAT3 phosphorylation in an organ culture of colonic tissue sections of wild-type mice after incubation with VEGF or PBS (Fig. 7 B). Interestingly, the addition of VEGF to the culture medium resulted in increased numbers of pSTAT3$^+$ epithelial cells in contrast to culture medium with PBS alone, suggesting the ability of VEGF to induce epithelial STAT3 activation in the colonic mucosa.

To show a functional relevance for VEGF-mediated STAT3 activation, we endoscopically injected VEGF into the colonic mucosa of mice with selective inactivation of STAT3 in IEC (STAT3 IEC KO mice) and wild-type mice exposed to the AOM+DSS protocol. 24 h after VEGF injection, we found an increased number of Ki67$^+$ epithelial cells in the colonic mucosa at the site of VEGF injection in wild-type, but not STAT3 IEC KO mice (Fig. 7, C and D). To verify a direct effect of VEGF stimulation on proliferation of IECs, we isolated IECs from STAT3 IEC KO and wild-type mice, and incubated these cells with VEGF. In these experiments, VEGF was able to significantly augment the proliferation of wild-type IECs, but not STAT3 KO IECs (Fig. 7 E).

To further characterize the functional consequences of increased proliferation of IECs in vivo, we endoscopically injected VEGF into tumors of STAT3 IEC KO mice and wild-type mice over a period of 2 wk. VEGF injection resulted in an increased tumor growth in wild-type mice, but not in STAT3 IEC KO mice (Fig. 7 F). Because of the tissue-specific deletion of STAT3 in IEC in STAT3 IEC KO mice, these differences indicate a direct effect of VEGF on tumor rather than endothelial cells.

IL-6 mediates the expression of VEGFR2 on colonic epithelial cells during chronic inflammation

Among several cytokines, IL-6 and TNF especially have been implicated in the pathogenesis of CAC (Becker et al., 2004; Popivanova et al., 2008; Bollrath et al., 2009; Grivennikov et al., 2009). To analyze the role of IL-6 and TNF during the up-regulation of VEGFR2 on epithelial cells, we exposed IL-6–deficient and TNFR1-/TNFR2-deficient mice, in comparison to wild-type mice, to AOM+DSS colitis. IL-6– and TNFR1-/TNFR2-deficient mice showed decreased tumor development in comparison to wild-type mice (unpublished data). Immunohistochemistry revealed reduced expression of VEGFR2 in colonic epithelial cells of IL-6–deficient mice, whereas the inflamed epithelium of TNFR1-/TNFR2-deficient and wild-type mice was positive for VEGFR2 (Fig. 8 A). Although VEGF levels were similar between wild-type and IL-6–deficient mice, Western blot analysis revealed a decreased expression of VEGFR2 in tumors of IL-6–deficient mice (Fig. 8 B).

Interestingly, IL-6 has been previously shown to induce the expression of VEGFR2 on endothelial cells in vitro (Yao et al., 2006). To test effects of IL-6 on IEC, we incubated colonic mucosa of wild-type animals with hyper-IL-6 (hIL-6), a fusion protein of IL-6 and soluble IL-6 receptor, in tissue culture experiments. hIL-6 treatment resulted in increased expression of VEGFR2 mRNA in the tissue specimens (Fig. 8 C). To further

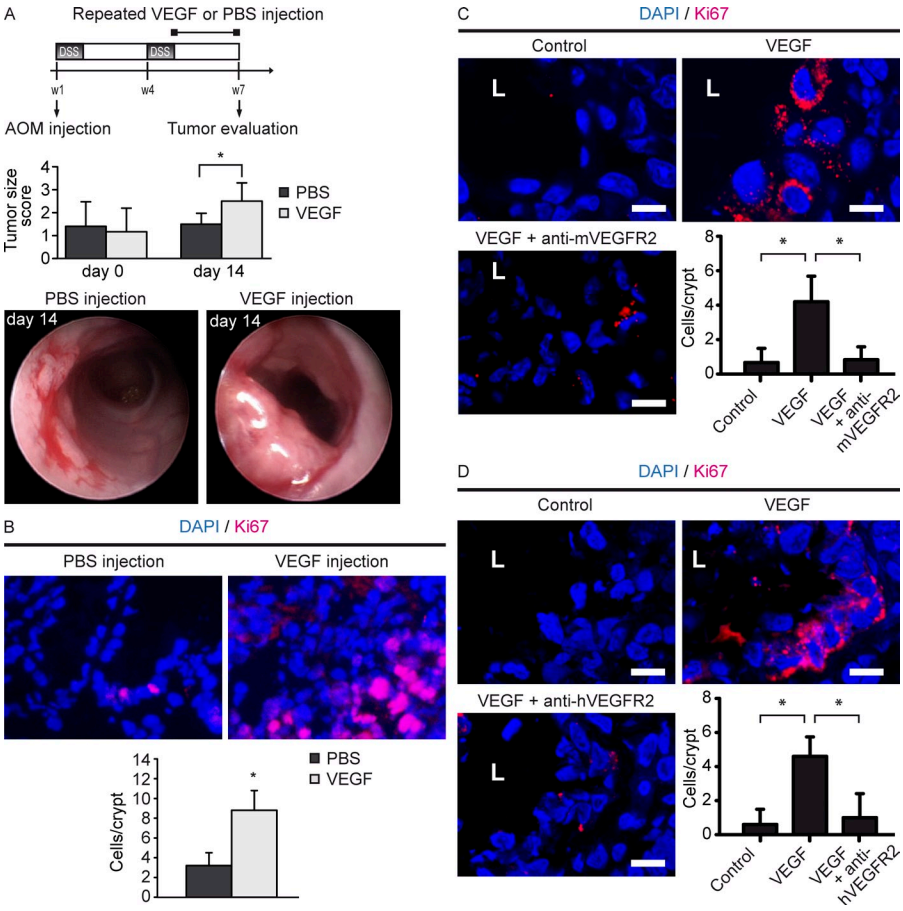

Figure 6. VEGF-mediated proliferation of IECs is dependent on VEGFR2 activation. (A) VEGF or PBS was injected endoscopically into growing tumors of AOM+DSS-treated animals 3 times per week. After 2 wk of repeated VEGF injections, tumor size was measured. Data show mean values ± SD (n = 5 per group) and represent two independent experiments. *, $P < 0.005$. (bottom) Endoscopic images are representative images at day 14 of VEGF and PBS injections. (B) Images show immunohistochemistry for Ki67 in mice treated as in A (top). Bar graphs show quantification of Ki67$^+$ tumor cells (bottom). Data represent mean values ± SD (n = 4 per group). The experiment was performed twice with similar results. *, $P < 0.01$. (C and D) Recombinant mouse or human VEGF (final concentration, 100 ng/ml) was added to inflamed colon specimens of AOM+DSS-treated mice (C) or endoscopic biopsies of human IBD patients (D). Proliferating epithelial cells were measured by Ki67 staining. Anti–mouse or anti–human blocking VEGFR2 antibodies were added where indicated. Representative images from three independent experiments per group are shown. *, $P < 0.05$. Bars, 10 µm.

analyze the ability of hIL-6 to induce VEGFR2 expression in vivo, we injected hIL-6 into the colonic mucosa of healthy mice. In comparison to the injection of PBS, hIL-6 resulted in an increased expression of VEGFR2 on IEC (Fig. 8 C), suggesting IL-6–dependent regulation of VEGFR2 signaling in vivo.

In a final series of studies, we aimed to demonstrate the direct effects of hIL-6 on VEGFR2 gene expression in IECs. In these experiments, we isolated IECs from VEGFR2 promoter luciferase reporter mice and control mice (purity >95%, as determined by E-Cadherin staining; Fig. 8 D). Subsequently, cells were stimulated for 3 h with hIL-6, followed by analysis of luciferase reporter gene activity. It was found that hIL-6 treatment leads to a significant increase of luminescence in IECs isolated from VEGFR2 promoter luciferase reporter mice (Fig. 8 E), indicating that IL-6 signaling drives VEGFR2 gene transcription in IECs.

DISCUSSION

Growing evidence supports an important link between chronic inflammation and tumor development. This is notably evident in patients with IBD such as Crohn's disease and ulcerative colitis, where the risk for CAC increases with the duration and severity of intestinal inflammation (Bernstein et al., 2001). However, although chronic gastrointestinal inflammation has been shown to increase epithelial proliferation (MacDonald, 1992) and antiinflammatory therapy has been shown to reduce cancer growth (Stolfi et al., 2008), the molecular mechanisms that lead to tumor development in chronic inflammation are only poorly understood. In this study, we show that patients with CAC, in contrast to sporadic CRC and control patients, have activated VEGFR2 on IECs. Notably, inhibition of VEGF signaling had a protective effect in a mouse model of CAC associated with a blockade of STAT3-dependent tumor cell proliferation in vivo, suggesting that VEGF signaling in IECs acts as a molecular link between inflammation and cancer development.

VEGF, which was initially described as vascular permeability factor (Senger et al., 1983), is an important regulator of angiogenesis through the initiation of vessel growth, the inhibition of endothelial cell apoptosis, and the incorporation of hematopoietic and endothelial progenitor cells into the developing vasculature (Ellis and Hicklin, 2008). After the approval of bevacizumab for the treatment of metastatic sporadic CRC, the inhibition of VEGF signaling has been applied to various types of cancer and several new therapeutics targeting this pathway have been developed, further supporting the important role of angiogenesis during tumor growth (Jain et al., 2006; Ferrara et al., 2007).

In our experiments, reduced tumor growth was paralleled by a decrease of intratumoral vessel density in anti-VEGF–treated animals, suggesting an effective inhibition of angiogenesis. Furthermore, we analyzed the normalization

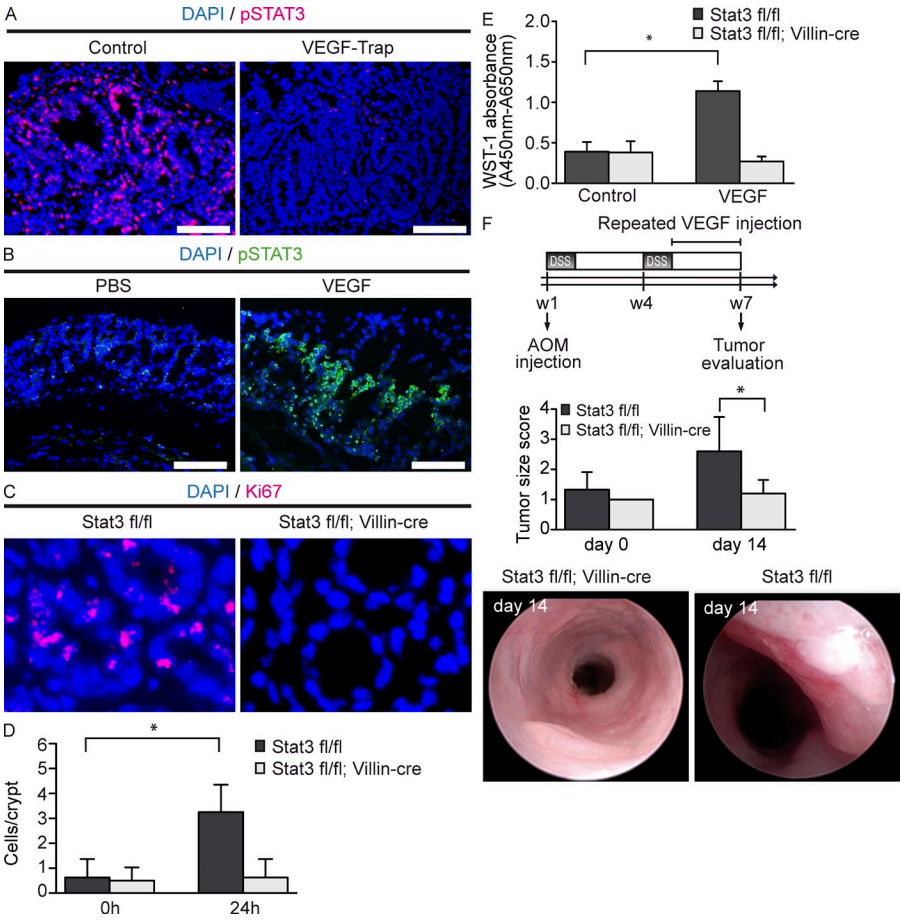

Figure 7. VEGF mediates tumor cell proliferation via STAT3 activation. (A) Immunohistochemistry of pSTAT3+ tumor cells in control or VEGF-Trap–treated animals. Representative images of four experiments subjected to AOM+DSS treatment. (B) VEGF (250 ng/ml) was added to a culture of colon tissue of wild-type mice. Phosphorylation of STAT3 was measured. Bars, 100 µm. Representative images from four independent experiments are shown. (C and D) VEGF (100 ng) was injected endoscopically into the mucosa of Stat3 fl/fl and Stat3 fl/fl + Villin-cre mice. Images show immunohistochemistry for Ki67 (C). Bar graphs show the number of Ki67+ cells 24 h later. (D) Data represent mean values ± SD (n = 4 per group). The experiment was performed twice with similar results. *, $P < 0.05$. (E) IECs (purity > 95%) were isolated from the inflamed colon of Stat3 fl/fl and Stat3 fl/fl + Villin-cre mice and subsequently stimulated with VEGF (final concentration, 100 ng/ml) in vitro. Proliferation of IECs was analyzed using the WST-1 proliferation assay after 3 h of VEGF incubation. Data represent mean values ± SD (n = 6 per group). Representative images from three independent experiments are shown. *, $P < 0.05$. (F) Stat3 fl/fl and Stat3 fl/fl + Villin-cre mice were exposed to AOM+DSS treatment. After 5 wk, VEGF (100 ng) was injected repeatedly into size-matched tumors of Stat3 fl/fl and Stat3 fl/fl + Villin-cre mice during a period of 14 d. Tumor growth was measured at indicated time points. Data are mean values ± SD (n = 5 per group). The experiment was performed twice with similar results. *, $P < 0.05$. Endoscopic pictures represent images of one representative animal per group.

of the tumoral vessel structure after antiangiogenic therapy with VEGF-Trap (Baish and Jain, 1998; Baish and Jain, 2000; Lin et al., 2008). The concept about a normalization of the tumor vasculature is based on a reversal of abnormal structures of tumor vessels at the microscopic level (Jain, 2005). To assess a possible normalization of the functional vascular morphology, we used confocal endoscopy in combination with optical contrast endoscopy of colonic vessels after i.v. injection of the plasma marker FITC-dextran and calculated the fractal dimension of the vessel network. Whereas the combination of conventional endoscopy with confocal endoscopy has been successfully used in patients for the in vivo detection of colonic neoplasia (Kiesslich et al., 2004), it has not been reported in mice so far and provides the advantage that the microvascular structure can be analyzed in living animals at several time points without the need to injure the animal. Furthermore, the confocal probe can be positioned directly next to relevant structure. By using optical contrast endoscopy and endomicroscopy, we noted normalization of vessel structure upon anti-VEGF therapy. Additionally, anti-VEGF therapy resulted in an increase of the microvascular fractal dimension, reflecting a more homogenous vascular network in tumors of treated animals. Therefore, we conclude that anti-VEGF therapy effectively reduces angiogenesis in experimental CAC.

Because growing evidence supports a role for angiogenesis in chronic inflammation and autoimmune disease (Carmeliet, 2003; Costa et al., 2007), the inhibition of VEGF-signaling has also been proposed as a promising therapeutic strategy in these disorders. In fact, several studies have shown beneficial effects for VEGF-blockade in animal models of chronic inflammation (Costa et al., 2007). With regard to IBD, Scaldaferri et al. (2009) showed that the inhibition of VEGF signaling in DSS colitis reduces inflammation, whereas the overexpression of VEGF leads to an augmentation of intestinal inflammation. These results were not only attributed to the role of angiogenesis during the inflammatory response, but also to an increased recruitment of leukocytes to the intestinal vascular endothelium. Whereas only limited data are available regarding the role of VEGF in intestinal inflammation, other studies, mainly on experimental models of arthritis, have shown several proinflammatory properties of VEGF, which include leukocyte migration, cytokine production, and Th1 cell differentiation (Grosios et al., 2004; Mor et al., 2004; Yoo et al., 2005). Therefore, we additionally evaluated inflammation in experimental CAC after anti-VEGF therapy. In contrast to the study by Scaldaferri et al. (2009), we

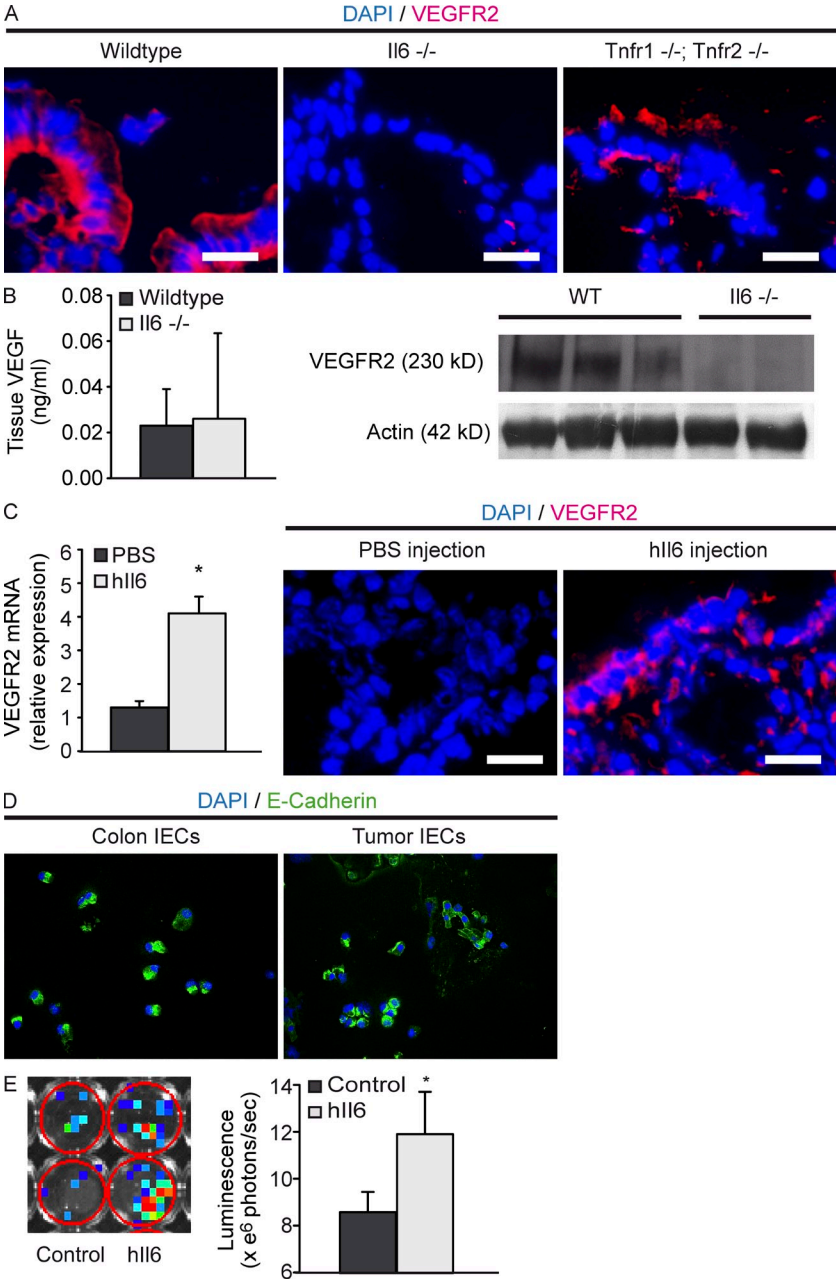

Figure 8. IL-6 induces the expression of VEGFR2 on epithelial cells as a tumor-promoting effect during chronic inflammation. (A) Immunohistochemistry of VEGFR2 in the inflamed epithelium of wild-type, IL-6–deficient, and TNFR-1–/TNFR-2–deficient mice. Representative images of four experiments. (B) Tissue levels of VEGF were measured in IL-6–deficient and wild-type mice by ELISA. VEGFR2-expression was measured by Western blot analysis. Actin was used as a loading control. The experiment was performed twice with similar results. (C) Wild-type colonic tissue was incubated with hIL-6 (10 ng/ml), and expression of VEGFR2 mRNA was measured by quantitative real-time PCR. Data represent mean values ± SD ($n = 4$ per group). The experiment was repeated twice with similar results. *, $P < 0.05$. VEGFR2 expression was measured by immunohistochemistry after endoscopic injection of hIL-6 (100 ng) into the mucosa of wild-type mice. Representative images from four experiments are shown. (D) Immunocytochemistry for E-Cadherin in isolated IECs from control colon and tumor tissue. Images are representative of four independent experiments. (E) Isolated IECs from VEGFR2 luciferase reporter mice were stimulated with hIL-6 (final concentration, 15 µg/ml) in vitro. After 3 h of stimulation, luminescence was measured using the IVIS Lumina II Imaging System. The total flux of photons per second was measured in each well. Data show mean values ± SD ($n = 6$ per group) and are representative for 3 independent experiments. *, $P < 0.05$. Bars, 20 µm.

could not observe an effect of VEGF inhibition on endoscopic colitis scores, which may be explained by the duration of the experimental procedure. Whereas Scaldaferri et al. (2009) evaluated the role of VEGF in a model of acute DSS colitis, we exposed experimental animals to several cycles of DSS, a protocol that is used for the study of chronic colitis (Strober et al., 2002; Neufert et al., 2007). These data suggest that VEGF signaling may be important in acute rather than chronic inflammation, at least in the intestine, and that the protective effect of anti-VEGF therapy on tumor development in our experiments cannot be explained by a direct effect on intestinal inflammation.

In addition to its role in angiogenesis and inflammation, some studies have proposed a direct effect of VEGF on tumor cells, which is derived from the detection of VEGF receptors on several lines of tumors (Jain et al., 2006; Ellis and Hicklin, 2008). Because VEGF induces survival, migration, and invasion of endothelial cells, the activation of VEGF receptors on tumor cells could mediate tumor growth and metastasis. In fact, a recent study by Lichtenberger et al. (2010) showed that VEGFR1 is up-regulated in a mouse model of spontaneous skin papillomas and in human squamous cell carcinomas and synergizes with EGFR to promote the proliferation of this skin neoplasm. Furthermore, in a study on the effect of bevacizumab in patients with inflammatory breast cancer, Wedam et al. (2006) found phosphorylated VEGFR2 on tumor cells with decreased numbers of $pVEGFR2^+$ tumor cells in patients treated with bevacizumab. The expression of VEGFR2 has also been shown on tumor cells from patients with CRC (Giatromanolaki et al., 2007). Nevertheless, a functional significance for VEGFR2 expression on tumor cells has not been shown so far. In the present study, we found an increased expression of total and phosphorylated VEGFR2, but not VEGFR1, in intratumoral epithelial cells of AOM+DSS-treated mice and in tumor cells of colitis-associated neoplasias of humans. Interestingly, VEGFR2 expression was also elevated in inflamed colonic epithelial

cells of AOM+DSS-treated mice and epithelial cells from tissue samples of patients with Crohn's disease and ulcerative colitis, whereas a relatively low VEGFR2 expression was noted on tumor cells in sporadic CRC, suggesting an inflammation-dependent up-regulation of VEGFR2 on IEC. Because tumors of VEGF-Trap–treated animals showed decreased numbers of proliferating tumor cells, we assumed a direct effect of VEGF signaling on tumor growth. This concept was further supported by an increased proliferation of tumor cells in vitro and in vivo through the administration of recombinant VEGF. Furthermore, proliferation of IECs could be suppressed by neutralizing anti-VEGFR2 antibodies, suggesting that the VEGF–VEGFR2 signaling pathway drives IEC proliferation in the AOM+DSS model. Interestingly, it has been shown in $APC^{\Delta 716}$ mice, a model resembling human familial adenomatous polyposis, that the vascular density in intestinal tumors increases only in tumors exceeding a diameter of 1 mm, and thus smaller tumors are not dependent on angiogenesis (Seno et al., 2002). Because we were able to detect tumors with a size >1 mm in diameter in contrast-enhanced endoscopy and the reduced tumor scores in anti-VEGF–treated animals were mainly dependent on reduced tumor numbers, anti-VEGF seemed to be more effective during early stages of tumor development, including tumor initiation and promotion, which do not rely on angiogenesis.

Because VEGFR2 was expressed on inflamed epithelial cells in AOM+DSS colitis and patients with IBD and CAC rather than sporadic CRC, we proposed that inflammation might lead to an up-regulation of VEGFR2 on epithelial cells and thereby promotes the proliferation of these cells as a possible link to tumor development. Consistently, IECs in AOM+DSS colitis and IBD patients showed increased proliferation as compared with controls.

Several recent studies have shown that the proinflammatory cytokine IL-6 directly acts on epithelial cells to induce the activation of signal transducer and activator of transcription 3 (STAT3) and thereby induces the proliferation of epithelial cells in AOM+DSS colitis (Becker et al., 2004; Bollrath et al., 2009; Grivennikov et al., 2009). Interestingly, IL-6 has also been shown to be a potent inducer of VEGFR2 expression on vascular endothelial cells (Yao et al., 2006). Thus, we analyzed the ability of IL-6 to induce the expression of VEGFR2 on IEC and noted that hyper-IL-6 induces VEGFR2 promoter activity in IECs. In addition, whereas the injection of hyper-IL-6 into the healthy colonic mucosa of wild-type mice resulted in an increased expression of VEGFR2 on epithelial cells, IL-6–deficient mice showed a reduced expression of VEGFR2 on epithelial cells in comparison to wild-type mice upon AOM+DSS colitis, indicating IL-6–dependent regulation of VEGFR2 expression. VEGFR2 activation on epithelial cells in turn leads to STAT3-dependent proliferation consistent with previous findings, indicating that VEGF can induce the phosphorylation of STAT3 on tumor cells in vitro (Lu et al., 2006). However, it remained to be determined whether activation of VEGFR2 on tumor cells has functional relevance in vivo. In the present study, we observed that VEGF was able to induce proliferation of tumor epithelial cells in wild-type mice, but not mice with selective inactivation of STAT3 in IEC, suggesting that VEGFR signaling controls tumor cell proliferation via STAT-3 activation in epithelial cells. Based on these findings it is tempting to speculate that the beneficial effect of anti-VEGF therapeutics in the presence of local inflammation is at least partially caused by direct anti-tumor effects via STAT-3.

Our data demonstrate that chronic intestinal inflammation leads to the up-regulation of VEGFR2 on epithelial cells and thereby sensitizes these cells to VEGF-mediated proliferation via STAT3 activation. Thus, VEGF signaling links chronic inflammation to tumor development in CAC through the regulation of angiogenesis and a direct tumor-promoting effect. Because VEGF has been implicated in the pathogenesis of chronic inflammatory disorders and our data suggest an involvement of VEGFR2 signaling in tumor initiation and promotion, anti-VEGF therapies might reduce the risk for tumor development in patients with IBDs. Furthermore, the expression of VEGF on tumor cells might be a prognostic marker for a successful therapy with anti-VEGF therapeutics.

MATERIALS AND METHODS

Animals and model of CAC. Specific pathogen–free C57BL/6 mice (8–10 mo old) were obtained from the central animal facility of Mainz and Erlangen. IL-6–deficient and TNF-R1– and R2-deficient mice were obtained from The Jackson Laboratory. STAT3 fl/fl mice were provided by S. Akira (Osaka University, Osaka, Japan) and crossed with villin-cre mice, which were received from D. Gumucio and B. Madison (University of Michigan Medical School, Ann Arbor, MI). STAT3 IEC KO mice have been previously described (Pickert et al., 2009). VEGF-luc transgenic mice and VEGFR2-luc transgenic mice were obtained from Caliper Life Sciences, Inc./Xenogen Corporation. CAC was induced as previously described (Neufert et al., 2007). In short, mice were injected with a single dose of the mutagenic agent 7.4 mg/kg AOM (Sigma-Aldrich), followed by three cycles of 2.5% DSS in drinking water for 1 wk and normal drinking water for 2 wk. The animal studies were conducted at the Universities of Mainz and Erlangen-Nuremberg and approved by the Institutional Animal Care and Use Committee of the University of Mainz and the State Government of Middle Franconia.

Patients. Paraffin-embedded intestinal specimens from patients with active IBD, CAC, and CRC were obtained from the Institute of Pathology (Bayreuth, Germany). Paraffin sections were made and stained with hematoxylin and eosin according to routine methods or used for immunohistochemistry as specified in the Immunohistochemistry section. Tissue culture experiments were performed with endoscopic biopsy specimens of IBD patients. The collection of biopsies was approved by the ethical committee and the institutional review board of the University of Erlangen-Nuremberg, and each patient gave written informed consent.

Narrow band imaging endoscopy, confocal in vivo endoscopy, multispectral fluorescence, and luminescence imaging. Repeated monitoring of tumorigenesis was performed with a high-definition narrow band imaging (NBI) endoscope (Exera II; Olympus) that was equipped with a 2-mm outer diameter optical probe (Storz). Endoscopy of mice and scoring of intestinal inflammation, tumor numbers, and tumor size was conducted as previously described (Becker et al., 2005). For detection of vessel morphology upon NBI endoscopy, single images were obtained and subsequently analyzed with ImageJ software at later time points (National Institutes of Health). Additionally, a fiber confocal microscope (FCM1000; Leica) with a 0.9-mm outer diameter probe was used for in vivo confocal endomicroscopy

of the microvascular architecture. The probe was fed through a manipulation sheath of the endoscope and positioned endoscopically to the area of interest. For the detection of vessel morphology, 100 µl of FITC-Dextran (70 kD, 5 mg/ml; Sigma-Aldrich) were injected into the tail vein of the experimental animal as a plasma marker and images were recorded for offline analysis.

Evaluation of the vessel structure including vessel density, mean vessel segment length, and fractal dimension of vessels, was performed with ImageJ software from recorded images of NBI-endoscopy and endomicroscopy (Fig. S3).

Multispectral fluorescence imaging of integrin $\alpha_v\beta_3$ was performed after injection of fluorescence imaging agent IntegriSense into the tail vein of selected experimental animals (100 µl per animal; VisEn Medical) with the Maestro imaging system (Intas).

Analysis of VEGF or VEGFR2 expression in VEGF-luc or VEGFR2-luc transgenic mice was performed at the indicated time points. Therefore, mice were analyzed with the IVIS Lumina II Imaging System (Caliper Life Sciences) 10 min after intraperitoneal injection of firefly luciferin (150 mg/kg; Promega).

Administration of VEGF-Trap, sVEGFR1, VEGF, and IL-6 in CAC. Treatment of C57BL/6 mice with VEGF-Trap, sVEGFR1, or VEGF was initiated after endoscopic detection of already established tumors at week 4 of the AOM+DSS protocol. Animals were then equally assigned to a treatment group and a control group to ensure matching tumor scores before the administration of each compound. VEGF-Trap (provided by Regeneron Pharmaceuticals Inc.) was injected subcutaneously 3 times per week at a dosage of 25 mg/kg for a duration of 4 wk. The control group received hFc (25 mg/kg). An adenoviral vector expressing sVEGFR1 has been previously described (Scaldaferri et al., 2009) and was injected into the tail vein at a concentration of 4 mg/kg. The control group received a control vector alone (LacZ) at a concentration of 4 mg/kg. In some experiments, VEGF was endoscopically injected into already established tumors or the mucosa (50–100 µl of a 1 µg/ml solution), whereas PBS was injected into tumors of control mice.

Hyper-IL-6 was generated as previously described (Fischer et al., 1997) and endoscopically injected into the colonic mucosa of untreated C57 BL/6 mice (100 µl of a 1 µg/ml solution).

Isolation of IECs and in vitro experiments. Tumors and tumor-free colons of wild-type or reporter gene mice were incubated at 37°C in HBSS containing 2 mM EDTA, 1 mM EGTA, and 1% FCS for 15 min to separate epithelial cells. Isolated cells were filtered through a 40-µm cell strainer (BD) and cultured at 37°C in complete RPMI 1640 medium.

To confirm the purity of the separation, IECs were fixed to glass slides in a Cytospin2-centrifuge (Shandon). After centrifugation at 500 rpm for 5 min, slides were removed and dried for 2 h. Immunohistochemistry for E-Cadherin was performed as described in the Immunohistochemistry section, and the ratio of E-Cadherin–positive cells was counted. A purity of >95% could be confirmed for IEC isolation from tumor and tumor-free tissue.

For the stimulation of IECs, mouse VEGF (Miltenyi Biotec) was added at a final concentration of 100 ng/ml to the culture medium; alternatively hIL-6 was added at a final concentration of 15 µg/ml. The analysis of IEC-proliferation was performed with the WST-1 cell proliferation reagent (Roche) according to the manufacturer's instructions. Luminescence of IECs from VEGFR2-luc transgenic mice was measured 10 min after addition of 150 mg/kg firefly luciferin (Promega) to the cell culture medium with the IVIS Lumina II Imaging System (Caliper Life Sciences) according to the manufacturer's instructions.

FACS analysis of isolated IECs. Epithelial cells from control colon tissue and tumor tissue of AOM+DSS-treated mice were isolated as described above. Analysis of VEGFR2 expression on epithelial cells by FACS was performed with FITC-labeled antibodies to E-Cadherin (eBioscience) and biotin-labeled antibodies to VEGFR2 (eBioscience). After antibody incubation at 4°C for 30 min, cells were washed with PBS/1% FCS. Subsequently, cells were incubated with streptavidin-Cy3 (Dianova) for 10 min and washed twice in PBS/1% FCS before FACS analysis, which was performed with the FACSCanto II System (BD).

Quantitative analysis of gene expression. Total RNA was isolated from cells and organs with RNeasy columns (QIAGEN), including DNase I digestion. cDNA was generated using the iScript cDNA Synthesis kit (Bio-Rad Laboratories). Quantitative real-time PCR analysis for VEGFR2 and HPRT was performed using specific QuantiTect Primer/Probe assays (QIAGEN) and QuantiTect Sybr Green (QIAGEN). The expression of VEGFR2 mRNA was analyzed in normal IECs, tumor IECs, and nonepithelial cells of healthy mucosa. Gene expression was calculated relative to the house-keeping gene β-actin using the ΔΔCt algorithm.

Protein isolation and ELISA. Plasma samples were prepared from whole blood obtained through cardiac puncture of experimental animals. Tissue protein was isolated from frozen colon and tumor specimens with the M-PER mammalian protein extraction reagent (Thermo Fisher Scientific). Protein concentration was analyzed using the Bradford protein assay.

For measurement of VEGF in plasma and tissues, we used a mouse VEGF-ELISA kit (Antigenix America Inc.) according to the manufacturer's instructions. Equal amounts of tissue protein lysates and plasma were used.

Western blot analysis. Western blotting was performed as previously described (Becker et al., 2003). In short, equal amounts of isolated protein (100 µg) were added to 12.5 µl of electrophoresis sample buffer (Roth) and boiled according to the manufacturer's guidelines. Proteins were separated by SDS-PAGE on precast gels (4–20% acrylamide; NuSep) and transferred to a nitrocellulose membrane, which was incubated with specific antibodies against VEGFR2 (dilution, 1/1,000; Cell Signaling Technology) and β-actin (dilution, 1/10,000; Cell Signaling Technology). Detection of specific bands was performed with the ECL Western blotting analysis system (PerkinElmer).

Histological analysis of colon cross sections. Tissues were isolated from mice, infused with 4% paraformaldehyde, and embedded in paraffin. Sections from these samples were stained with hematoxylin and eosin. The degree of inflammation was graded semiquantitatively on a scale from 0–6 combined of inflammatory cell infiltration ranging from 0–3 and tissue damage ranging from 0–3 (Neurath et al., 2002; Mudter et al., 2008).

Immunohistochemistry. Cryosections were made of frozen tissue specimens, fixed with 4% paraformaldehyde, and sequentially incubated with methanol, avidin/biotin (Vector Laboratories), and protein-blocking reagent (Dako). Primary antibodies specific for CD31 (initial concentration, 0.5 mg/ml; dilution, 1/500; eBioscience), E-Cadherin (initial concentration, 0.5 mg/ml; dilution, 1/200; eBioscience), VEGFR2 (dilution, 1/500; Cell Signaling; Abcam; eBioscience), phosphoVEGFR2 (dilution, 1/500; Cell Signaling Abcam), pSTAT3 (dilution: 1/500; Cell Signaling), myeloperoxidase (initial concentration, 2 mg/ml; dilution, 1/20; Abcam), F4/80 (initial concentration, 0.5 mg/ml; dilution, 1/500; BD), CD4 (dilution, 1/200; BD), and Ki67 (dilution, 1/200; Dako) were dissolved in TBST/0.5% BSA and incubated overnight at 4°C. For negative controls, the primary antibody was omitted. In the case of VEGFR2 and pVEGFR2, additional negative controls were performed by administration of the blocking peptide during primary antibody incubation (VEGFR2 and pVEGFR2; dilution, 1/10; Cell Signaling Technology), furthermore, anti-VEGFR2 and -pVEGFR2 antibodies from different manufacturers were tested to ensure specificity. Subsequently, slides were incubated with biotinylated secondary antibodies and streptavidin-HRP and stained with Tyramide (Cy3 and FITC) according to the manufacturer's guidelines (PerkinElmer). Nuclei were counterstained with DAPI contained in Vectashield mounting medium (Vector Laboratories). Next, brightfield (IX70; Olympus) or confocal microscopy (SP5; Leica) was performed. Quantification of positive cells was performed with ImageJ software (National Institutes of Health) and counted per longitudinal crypt.

In vitro organ culture. Intestinal tumors, mucosal sections of experimental animals or colonic biopsies of patients with IBD were placed on steel grids in an organ culture chamber at 37°C with a 95% O_2/5% CO_2 atmosphere in

RRMI1640 medium (with 10% fetal calf serum, 1% glutamine, 1% streptomycin, and 1% penicillin). Recombinant mouse VEGF-A (final concentration, 100 ng/ml; Milteny Biotec) or human VEGF-A (final concentration, 100 ng/ml; Milteny Biotec) and mouse or human anti-VEGFR2 antibodies (final concentration, 10 µg/ml; R&D Systems) were added to the culture medium. After the incubation period of 12 h, tissue samples were prepared for immunohistological examination as described in the previous section.

Statistical analysis. All data comparing two groups were analyzed with the Student's *t* test using "R: A Language and Environment for Statistical Computing" (http://www.r-project.org/). Data comparing more than two groups were analyzed with the Kruskal-Wallis test followed by Dunn's test with GraphPad Prism v 5.00.

Online supplemental material. Fig. S1 shows mRNA expression of VEGFR2 in tumor cells, IECs, and colon non-IECs; controls for VEGFR2 immunohistochemistry; and immunohistochemistry for VEGFR1 in mouse and human tissue samples. In Fig. S2, immunohistochemical double staining for VEGF and various cell types in mouse tissue samples and staining for VEGF in human tissue samples are demonstrated. Fig. S3 shows images from conventional and optical contrast endoscopy, images from in vivo fluorescence imaging for integrin $\alpha_v\beta_3$ in AOM+DSS-treated animals, confocal endoscopy of the microvasculature, and the calculation of the fractal dimension. Fig. S4 shows the number of Ki67-positive IECs in tissue samples from control patients, patients with IBD, CAC, and CRC. Online supplemental material is available at http://www.jem.org/cgi/content/full/jem.20100438/DC1.

M.F. Neurath and M.J. Waldner were supported by DFG within the Graduiertenkolleg GK 1043; M.F. Neurath, S. Wirtz, and C. Becker were supported by the DFG within the FOR527. M.F. Neurath received funding from the European Community's seventh Framework Programme (FP7/2007-2013) under grant agreement no. 202230, acronym GENINCA. M.F. Neurath was supported by the United European Gastroenterology Foundation Research Prize.

All authors declare no conflicting financial interests.

Submitted: 3 March 2010
Accepted: 4 October 2010

REFERENCES

Avraamides, C.J., B. Garmy-Susini, and J.A. Varner. 2008. Integrins in angiogenesis and lymphangiogenesis. *Nat. Rev. Cancer.* 8:604–617. doi:10.1038/nrc2353

Baish, J.W., and R.K. Jain. 1998. Cancer, angiogenesis and fractals. *Nat. Med.* 4:984. doi:10.1038/1952

Baish, J.W., and R.K. Jain. 2000. Fractals and cancer. *Cancer Res.* 60: 3683–3688.

Balkwill, F., K.A. Charles, and A. Mantovani. 2005. Smoldering and polarized inflammation in the initiation and promotion of malignant disease. *Cancer Cell.* 7:211–217. doi:10.1016/j.ccr.2005.02.013

Becker, C., S. Wirtz, M. Blessing, J. Pirhonen, D. Strand, O. Bechthold, J. Frick, P.R. Galle, I. Autenrieth, and M.F. Neurath. 2003. Constitutive p40 promoter activation and IL-23 production in the terminal ileum mediated by dendritic cells. *J. Clin. Invest.* 112:693–706.

Becker, C., M.C. Fantini, C. Schramm, H.-A. Lehr, S. Wirtz, A. Nikolaev, J. Burg, S. Strand, R. Kiesslich, S. Huber, et al. 2004. TGF-beta suppresses tumor progression in colon cancer by inhibition of IL-6 trans-signaling. *Immunity.* 21:491–501. doi:10.1016/j.immuni.2004.07.020

Becker, C., M.C. Fantini, S. Wirtz, A. Nikolaev, R. Kiesslich, H.A. Lehr, P.R. Galle, and M.F. Neurath. 2005. In vivo imaging of colitis and colon cancer development in mice using high resolution chromoendoscopy. *Gut.* 54:950–954. doi:10.1136/gut.2004.061283

Bernstein, C.N., J.F. Blanchard, E. Kliewer, and A. Wajda. 2001. Cancer risk in patients with inflammatory bowel disease: a population-based study. *Cancer.* 91:854–862. doi:10.1002/1097-0142(20010215)91:4<854::AID-CNCR1073>3.0.CO;2-Z

Bollrath, J., T.J. Phesse, V.A. von Burstin, T. Putoczki, M. Bennecke, T. Bateman, T. Nebelsiek, T. Lundgren-May, O. Canli, S. Schwitalla, et al. 2009. gp130-mediated Stat3 activation in enterocytes regulates cell survival and cell-cycle progression during colitis-associated tumorigenesis. *Cancer Cell.* 15:91–102. doi:10.1016/j.ccr.2009.01.002

Boquoi, A., R. Jover, T. Chen, M. Pennings, and G.H. Enders. 2009. Transgenic expression of VEGF in intestinal epithelium drives mesenchymal cell interactions and epithelial neoplasia. *Gastroenterology.* 136:596–606: e4. doi:10.1053/j.gastro.2008.10.028

Cao, Y. 2009. Positive and negative modulation of angiogenesis by VEGFR1 ligands. *Sci. Signal.* 2:re1. doi:10.1126/scisignal.259re1

Carmeliet, P. 2003. Angiogenesis in health and disease. *Nat. Med.* 9:653–660. doi:10.1038/nm0603-653

Chen, S.H., D.A. Murphy, W. Lassoued, G. Thurston, M.D. Feldman, and W.M. Lee. 2008. Activated STAT3 is a mediator and biomarker of VEGF endothelial activation. *Cancer Biol. Ther.* 7:1994–2003.

Clevers, H. 2004. At the crossroads of inflammation and cancer. *Cell.* 118:671–674. doi:10.1016/j.cell.2004.09.005

Costa, C., J. Incio, and R. Soares. 2007. Angiogenesis and chronic inflammation: cause or consequence? *Angiogenesis.* 10:149–166. doi:10.1007/s10456-007-9074-0

Ellis, L.M., and D.J. Hicklin. 2008. VEGF-targeted therapy: mechanisms of anti-tumour activity. *Nat. Rev. Cancer.* 8:579–591. doi:10.1038/nrc2403

Emura, F., Y. Saito, and H. Ikematsu. 2008. Narrow-band imaging optical chromocolonoscopy: advantages and limitations. *World J. Gastroenterol.* 14:4867–4872. doi:10.3748/wjg.14.4867

Ferrara, N. 2009. Vascular endothelial growth factor. *Arterioscler. Thromb. Vasc. Biol.* 29:789–791. doi:10.1161/ATVBAHA.108.179663

Ferrara, N., R.D. Mass, C. Campa, and R. Kim. 2007. Targeting VEGF-A to treat cancer and age-related macular degeneration. *Annu. Rev. Med.* 58:491–504. doi:10.1146/annurev.med.58.061705.145635

Fischer, M., J. Goldschmitt, C. Peschel, J.P. Brakenhoff, K.J. Kallen, A. Wollmer, J. Grötzinger, and S. Rose-John. 1997. I. A bioactive designer cytokine for human hematopoietic progenitor cell expansion. *Nat. Biotechnol.* 15:142–145. doi:10.1038/nbt0297-142

Folkman, J. 1971. Tumor angiogenesis: therapeutic implications. *N. Engl. J. Med.* 285:1182–1186. doi:10.1056/NEJM197108122850711

Giatromanolaki, A., M.I. Koukourakis, E. Sivridis, G. Chlouverakis, E. Vourvouhaki, H. Turley, A.L. Harris, and K.C. Gatter. 2007. Activated VEGFR2/KDR pathway in tumour cells and tumour associated vessels of colorectal cancer. *Eur. J. Clin. Invest.* 37:878–886. doi:10.1111/j.1365-2362.2007.01866.x

Grivennikov, S., E. Karin, J. Terzic, D. Mucida, G.Y. Yu, S. Vallabhapurapu, J. Scheller, S. Rose-John, H. Cheroutre, L. Eckmann, and M. Karin. 2009. IL-6 and Stat3 are required for survival of intestinal epithelial cells and development of colitis-associated cancer. *Cancer Cell.* 15:103–113. doi:10.1016/j.ccr.2009.01.001

Grosios, K., J. Wood, R. Esser, A. Raychaudhuri, and J. Dawson. 2004. Angiogenesis inhibition by the novel VEGF receptor tyrosine kinase inhibitor, PTK787/ZK222584, causes significant anti-arthritic effects in models of rheumatoid arthritis. *Inflamm. Res.* 53:133–142. doi:10.1007/s00011-003-1230-4

Grothey, A., and E. Galanis. 2009. Targeting angiogenesis: progress with anti-VEGF treatment with large molecules. *Nat. Rev. Clin. Oncol.* 6:507–518. doi:10.1038/nrclinonc.2009.110

Jain, R.K. 2005. Normalization of tumor vasculature: an emerging concept in antiangiogenic therapy. *Science.* 307:58–62. doi:10.1126/science.1104819

Jain, R.K., D.G. Duda, J.W. Clark, and J.S. Loeffler. 2006. Lessons from phase III clinical trials on anti-VEGF therapy for cancer. *Nat. Clin. Pract. Oncol.* 3:24–40. doi:10.1038/ncponc0403

Kerbel, R.S. 2008. Tumor angiogenesis. *N. Engl. J. Med.* 358:2039–2049. doi:10.1056/NEJMra0706596

Kiesslich, R., J. Burg, M. Vieth, J. Gnaendiger, M. Enders, P. Delaney, A. Polglase, W. McLaren, D. Janell, S. Thomas, et al. 2004. Confocal laser endoscopy for diagnosing intraepithelial neoplasias and colorectal cancer in vivo. *Gastroenterology.* 127:706–713. doi:10.1053/j.gastro.2004.06.050

Lichtenberger, B.M., P.K. Tan, H. Niederleithner, N. Ferrara, P. Petzelbauer, and M. Sibilia. 2010. Autocrine VEGF signaling synergizes with EGFR in tumor cells to promote epithelial cancer development. *Cell.* 140:268–279. doi:10.1016/j.cell.2009.12.046

Lin, K.Y., M. Maricevich, N. Bardeesy, R. Weissleder, and U. Mahmood. 2008. In vivo quantitative microvasculature phenotype imaging of healthy and malignant tissues using a fiber-optic confocal laser microprobe. *Transl. Oncol.* 1:84-94.

Lu, W., H. Chen, F. Yel, F. Wang, and X. Xie. 2006. VEGF induces phosphorylation of STAT3 through binding VEGFR2 in ovarian carcinoma cells in vitro. *Eur. J. Gynaecol. Oncol.* 27:363–369.

MacDonald, T.T. 1992. Epithelial proliferation in response to gastrointestinal inflammation. *Ann. N. Y. Acad. Sci.* 664:202–209. doi:10.1111/j.1749-6632.1992.tb39761.x

Mor, F., F.J. Quintana, and I.R. Cohen. 2004. Angiogenesis-inflammation cross-talk: vascular endothelial growth factor is secreted by activated T cells and induces Th1 polarization. *J. Immunol.* 172:4618–4623.

Mudter, J., L. Amoussina, M. Schenk, J. Yu, A. Brustle, B. Weigmann, R. Atreya, S. Wirtz, C. Becker, A. Hoffman, I. Atreya, S. Blesterfield, P.R. Galle, H. Lehr, S. Rose-John, C. Mueller, M. Lohoff, and M.F. Neurath. 2008. The transcription factor IFN regulatory factor-4 controls experimental colitis in mice via T cell-derived IL-6. *J. Clin. Invest.* 118:2415–2428.

Neufert, C., C. Becker, and M.F. Neurath. 2007. An inducible mouse model of colon carcinogenesis for the analysis of sporadic and inflammation-driven tumor progression. *Nat. Protoc.* 2:1998–2004. doi:10.1038/nprot.2007.279

Neurath, M.F., B. Weigmann, S. Finotto, J. Glickman, E. Nieuwenhuis, H. Iijima, A. Mizoguchi, E. Mizoguchi, J. Mudter, P.R. Galle, A. Bhan, F. Autschbach, B.M. Sullivan, S.J. Szabo, L.H. Glimcher, and R.S. Blumberg. 2002. The transcription factor T-bet regulates mucosal T cell activation in experimental colitis and Crohn's disease. *J. Exp. Med.* 195:1129–1143.

Pickert, G., C. Neufert, M. Leppkes, Y. Zheng, N. Wittkopf, M. Warntjen, H.-A. Lehr, S. Hirth, B. Weigmann, S. Wirtz, et al. 2009. STAT3 links IL-22 signaling in intestinal epithelial cells to mucosal wound healing. *J. Exp. Med.* 206:1465–1472. doi:10.1084/jem.20082683

Pitot, H.C. 1993. The molecular biology of carcinogenesis. *Cancer.* 72:962–970. doi:10.1002/1097-0142(19930801)72:3+<962::AID-CNCR2820721303>3.0.CO;2-H

Popivanova, B.K., K. Kitamura, Y. Wu, T. Kondo, T. Kagaya, S. Kaneko, M. Oshima, C. Fujii, and N. Mukaida. 2008. Blocking TNF-alpha in mice reduces colorectal carcinogenesis associated with chronic colitis. *J. Clin. Invest.* 118:560–570.

Scaldaferri, F., S. Vetrano, M. Sans, V. Arena, G. Straface, E. Stigliano, A. Repici, A. Sturm, A. Malesci, J. Panes, et al. 2009. VEGF-A links angiogenesis and inflammation in inflammatory bowel disease pathogenesis. *Gastroenterology.* 136:585–595: e5. doi:10.1053/j.gastro.2008.09.064

Semenza, G.L. 2003. Targeting HIF-1 for cancer therapy. *Nat. Rev. Cancer.* 3:721–732. doi:10.1038/nrc1187

Senger, D.R., S.J. Galli, A.M. Dvorak, C.A. Perruzzi, V.S. Harvey, and H.F. Dvorak. 1983. Tumor cells secrete a vascular permeability factor that promotes accumulation of ascites fluid. *Science.* 219:983–985. doi:10.1126/science.6823562

Seno, H., M. Oshima, T.O. Ishikawa, H. Oshima, K. Takaku, T. Chiba, S. Narumiya, and M.M. Taketo. 2002. Cyclooxygenase 2- and prostaglandin E(2) receptor EP(2)-dependent angiogenesis in Apc(Delta716) mouse intestinal polyps. *Cancer Res.* 62:506–511.

Shibuya, M., and L. Claesson-Welsh. 2006. Signal transduction by VEGF receptors in regulation of angiogenesis and lymphangiogenesis. *Exp. Cell Res.* 312:549–560. doi:10.1016/j.yexcr.2005.11.012

Stolfi, C., R. Pellegrini, E. Franze, F. Pallone, and G. Monteleone. 2008. Molecular basis of the potential of mesalazine to prevent colorectal cancer. *World J. Gastroenterol.* 14:4434–4439. doi:10.3748/wjg.14.4434

Strober, W., I.J. Fuss, and R.S. Blumberg. 2002. The immunology of mucosal models of inflammation. *Annu. Rev. Immunol.* 20:495–549. doi:10.1146/annurev.immunol.20.100301.064816

Wedam, S.B., J.A. Low, S.X. Yang, C.K. Chow, P. Choyke, D. Danforth, S.M. Hewitt, A. Berman, S.M. Steinberg, D.J. Liewehr, et al. 2006. Antiangiogenic and antitumor effects of bevacizumab in patients with inflammatory and locally advanced breast cancer. *J. Clin. Oncol.* 24:769–777. doi:10.1200/JCO.2005.03.4645

Yao, J.S., W. Zhai, W.L. Young, and G.Y. Yang. 2006. Interleukin-6 triggers human cerebral endothelial cells proliferation and migration: the role for KDR and MMP-9. *Biochem. Biophys. Res. Commun.* 342:1396–1404. doi:10.1016/j.bbrc.2006.02.100

Yoo, S.A., D.G. Bae, J.W. Ryoo, H.R. Kim, G.S. Park, C.S. Cho, C.B. Chae, and W.U. Kim. 2005. Arginine-rich anti-vascular endothelial growth factor (anti-VEGF) hexapeptide inhibits collagen-induced arthritis and VEGF-stimulated productions of TNF-alpha and IL-6 by human monocytes. *J. Immunol.* 174:5846–5855.

Yoo, S.A., S.K. Kwok, and W.U. Kim. 2008. Proinflammatory role of vascular endothelial growth factor in the pathogenesis of rheumatoid arthritis: prospects for therapeutic intervention. *Mediators Inflamm.* 2008:129873. doi:10.1155/2008/129873

Zisman, T.L., and D.T. Rubin. 2008. Colorectal cancer and dysplasia in inflammatory bowel disease. *World J. Gastroenterol.* 14:2662–2669. doi:10.3748/wjg.14.2662